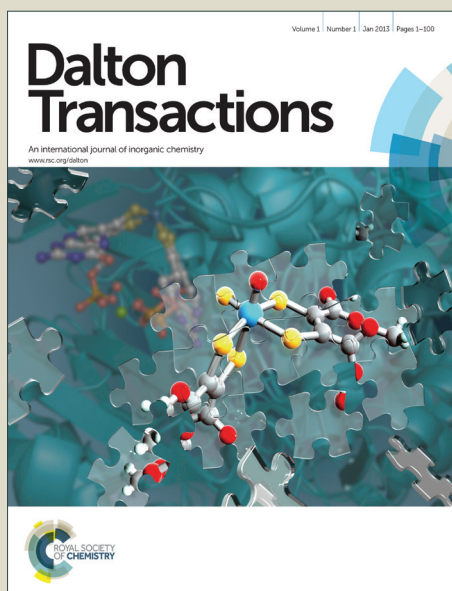


Dalton Transactions

Accepted Manuscript



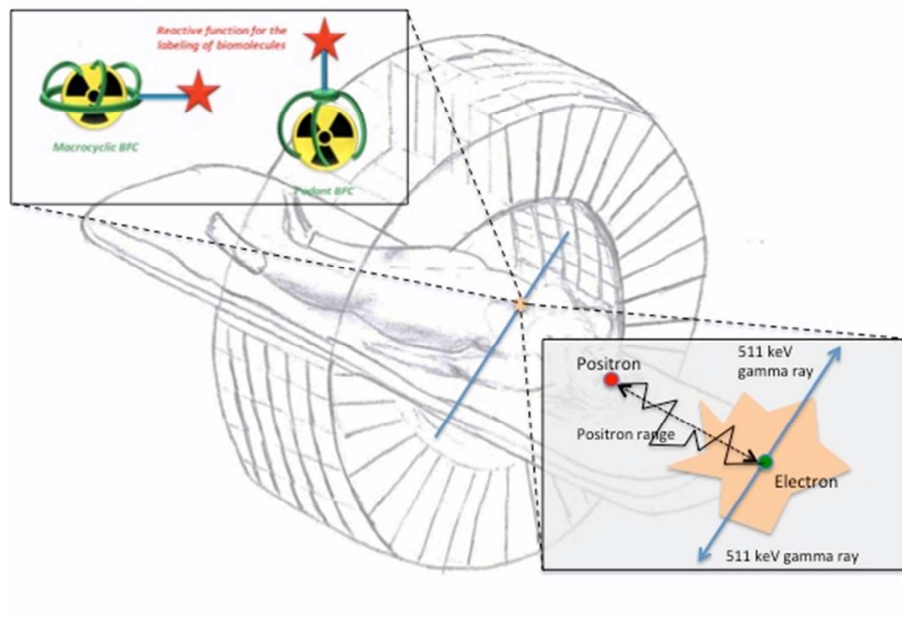
This is an *Accepted Manuscript*, which has been through the Royal Society of Chemistry peer review process and has been accepted for publication.

Accepted Manuscripts are published online shortly after acceptance, before technical editing, formatting and proof reading. Using this free service, authors can make their results available to the community, in citable form, before we publish the edited article. We will replace this *Accepted Manuscript* with the edited and formatted *Advance Article* as soon as it is available.

You can find more information about *Accepted Manuscripts* in the [Information for Authors](#).

Please note that technical editing may introduce minor changes to the text and/or graphics, which may alter content. The journal's standard [Terms & Conditions](#) and the [Ethical guidelines](#) still apply. In no event shall the Royal Society of Chemistry be held responsible for any errors or omissions in this *Accepted Manuscript* or any consequences arising from the use of any information it contains.

The use of radiometal isotopes in Positron Emission Tomography: a new nuclear imaging success story?



Radiometals: Towards a New Success Story in Nuclear Imaging?

David Brasse*^{a,c}, and Aline Nonat^{b,c}

Several limitations of ^{18}F and other non-metallic isotopes have been emphasized by the development of macromolecular biotargeting agents for cancer, including peptides, antibodies, fragments and oligonucleotides, which typically have biological half-lives that are much longer than the radioactive half-life of ^{18}F . Based on the ^{18}F -FDG success story, we can wonder whether all critical criteria are or can be fulfilled for the radiometallated bioconjugates to break through and which metals have the best chance for success. In this paper we give a brief overview of radiometal isotopes having the potential for PET imaging in term of physical properties, production capacity and associated chemistry.

A Introduction

The year 2000 represents an important milestone in nuclear imaging. The same year, the PET/CT was declared “image of the year” by the society of nuclear medicine, “invention of the year” by Time magazine and “outstanding basic science paper” for the work of Thomas Beyer *et al*¹ in the journal of Nuclear Medicine. As claimed by Johannes Czerning in 2003, the PET/CT was a technical evolution that has led to a medical revolution. The number of PET or PET/CT procedures in US was closed to 0.2 Million in 2000 and reached 1.85 Millions in 2012. We observe the same behaviour in Europe with a 21% increase of procedures between 2005 and 2010. This current success story as an invaluable tool in clinical routine is due to the concomitance of several factors, among which improvement in detector performance has in fact played a rather minor role.² The need for a “technetium”-like isotope for PET was mandatory. With a half-life of almost two hours and ideal physical properties for PET imaging, ^{18}F rapidly became the isotope of choice. However, it requires a well-established network of cyclotron facilities capable of providing radiolabelled compounds at the patient bed. Finding the clinical niche in which PET does not to compete but rather complement other imaging modalities was also a determining factor for the success of PET. The combination with CT promoted PET as the dominant tool in oncology.

Nuclear medical imaging is currently preparing for a new turning point in its history. Several limitations of ^{18}F and other non-metallic isotopes have been emphasized by the development of macromolecular biotargeting agents for cancer, including peptides, antibodies, fragments and oligonucleotides, which typically have biological half-lives that are much longer than the radioactive half-life of ^{18}F and ^{11}C . Furthermore, radiochemistry with non-metallic isotopes often necessitates demanding and complex synthesis with conditions that are not always compatible with these sensitive biomolecular agents. Based on the ^{18}F -FDG success story, we can wonder whether all critical criteria are or can be fulfilled for the radiometallated bioconjugates to break through and which metals have the best chance for success.

One determining factor is probably the way the isotopes are produced (reactor, cyclotron), packaged (radio-labelled molecules, generators) and distributed. The second item is highly correlated to their coordination chemistry and the availability of bifunctional chelators which can form stable and kinetically inert complexes in bio-friendly conditions and also be covalently attached to targeting vectors.³ We also need to

define the “killer applications” for which the added value is well identified compared to other approaches. Some exciting results have been already published in theranostic, multimodality approaches and boron neutron capture applications.⁴

Although the performance of the imaging modalities played a minor role in the FDG PET/CT success, we will present some advances in PET instrumentation and detector module.

B Availability of metal ions

B.1 Radiometals for PET

All nuclear medicine procedures require the use of radionuclides to highlight for example a functional disorder or to transfer enough energy to locally damage cancer cells. Over the last decades, nuclear physics facilities brought to our knowledge more than one hundred radioactive isotopes with properties useful for nuclear medicine.

The radioactive isotope is categorized according to its type of ionizing radiation. Gamma and positrons emitters will be used for imaging procedures while beta, alpha and electron are used for therapy purposes.

Several important criteria will push forward a radionuclide if its properties are well adapted to the medical application of interest. For example, its half-life should be long enough to be distributed and reach the target after the patient injection but short enough to minimize the patient exposure after the imaging procedure was performed. It should be long enough regarding the time required to transport the product between the production site and the examination room but short enough to prevent long-term waste-handling issues for the hospital.

Positron emission tomography (PET) imaging system are optimized to detect the two 511 keV photons coming from the annihilation of the positron. Prior to the annihilation, the unstable atom loses energy by emitting ionizing radiation. Depending on the isotope, the positrons that represent a fraction of the total amount of decays (branching ratio) are emitted according to a continuous kinetic energy spectrum defined by a maximum available energy.

The emitted charged particle loses its initial energy by collisions with the atoms in the surrounding tissue. Once the positron energy becomes sufficiently small, the particle collides with a free electron producing two photons almost 180° opposed. The distance travelled by the positron before the annihilation is called the positron range and depends on the initial energy of the particle. The properties required to become a good PET candidate are then a high branching ratio (BR) to optimize the injected activity, a low positron energy to limit the particle range and optimize the spatial resolution, a suitable half-life and appropriate chemical properties. The positron range can be computed from an empirical formula given by Katz and Penfold⁴.

$$R_{\max} \left[\frac{g}{\text{cm}^2} \right] = \begin{cases} 0.412E_{\beta}^{1.265-0.0954\ln(E_{\beta})} & 0.01 \leq E_{\beta} \leq 2.5 \text{ MeV} \\ 0.530E_{\beta} - 0.106 & E_{\beta} > 2.5 \text{ MeV} \end{cases} \quad (1)$$

where E_{β} represents the positron energy. In order to retrieve the distance travelled by the particle, the range has to be divided by the tissue density. Similarly to ^{99m}Tc for SPECT, ¹⁸F presents all the properties to rapidly become at the beginning of PET imaging the isotope of choice. It has a branching ratio close to 100% with a short average range in soft tissue of 0.6 mm but probably suffer from a short half-life of only two hours when macromolecules required more time to reach their biological target. To overcome this handicap, radiometal isotopes presenting longer half-lives can be used. Possible candidates for PET imaging are listed in Table 1.

Few elements present a positron energy allowing a range below 1 mm in soft tissue. This criteria may become important when preclinical studies are concerned but less penalizing when investigations at the organ scale are required.

If we consider the branching ratio of ¹⁸F as the gold standard and in order to obtain the same “image quality”, the amount of activity required when using ⁶⁴Cu, ⁸⁹Zr and ⁸⁶Y should be 5.5, 3 and 4.3 times higher than the one used with ¹⁸F. However, more information is required to correctly estimate the excess dose delivered to the patient such as the physical and biological half-lives, the biodistribution of the compound, the energy of the positron and the additional gamma rays.

For example, if we consider the external dose delivered by the gammas and the radiotoxicity reported in nuclide safety datasheets, we obtain lower values for ⁶⁴Cu than ¹⁸F (3.6×10⁻⁵ mSv/h for ⁶⁴Cu and 1.9×10⁻⁴ mSv/h for ¹⁸F per MBq at 1 meter for the external dose and 1.26×10⁻¹⁰ Sv/Bq for ⁶⁴Cu and 2.9×10⁻¹⁰ Sv/Bq for ¹⁸F in term of radiotoxicity when the product is ingested). In that case the excess dose delivered to the patient is mainly dictated by the low branching ratio of ⁶⁴Cu.

Taking into account all these considerations, 3 to 4 radiometals present interesting properties for PET imaging. Interest in using ⁶⁸Ga for clinical PET comes from its availability from a generator. While the positron range of ⁶⁸Ga is higher than the one of ¹⁸F and its half-life is around one hour, the availability of ⁶⁸Ga from a ⁶⁸Ge/⁶⁸Ga generator eliminates the need of an onsite cyclotron and makes ⁶⁸Ga an attractive alternative to ¹⁸F. ⁶⁴Cu seems to present appropriate properties to target macromolecules requiring longer half-life. We will have to keep in mind its low branching ratio and the emission of an additional beta minus particle (38.5%) with a maximum and average energy of 579 keV and 191 keV respectively. For longer half-lives, two radiometals present interesting properties: ⁸⁹Zr and ⁷¹As. While ⁸⁹Zr is well documented

and recognized to label compounds with long blood circulation, ^{71}As presents approximately the same half-life but a lower positron range, a higher branching ratio and an additional gamma ray with a lower energy.

Table 1: Radiometal isotopes potentially useful for PET imaging. β and γ stand for beta and gamma rays. BR stands for branching ratio and gives the number of emitted positrons relative to the total number of decays. I gives the number of emitted gamma rays relative to the total number of decays. For γ emission, only the most abundant gamma lines are listed.

	Half-life	β^+ emission (MeV)			γ emission (keV)		Positron range (mm)	
	hour	max	mean	BR (%)	photon	I (%)	max	mean
F-18	1.83	0.63	0.25	96.7	511	193	2.1	0.5
Cu-62	0.17	2.94	1.32	97.6	511	196	13.7	5.5
Cu-64	12.7	0.65	0.28	17.6	511	35	2.2	0.7
					1350	0.6		
Ga-68	1.13	1.90	0.84	87.7	511	178	8.4	3.1
Rb-82	0.02	3.38	1.53	81.8	511	191	15.9	6.5
		2.60	1.17	13.1			12.0	4.7
Y-86	14.7	1.22	0.53	11.9	511	64	5.0	1.7
					628	33		
					1077	83		
					1153	31		
					1854	17		
					1921	21		
Zr-89	78.4	0.90	0.39	22.7	511	45	3.4	1.1
					909	99		
As-71	65.3	0.82	0.35	27.9	511	57	3.0	0.9
					175	82		
As-72	26,0	2.50	1.12	64.2	511	176	11.5	4.5
					834	81		
As-74	426.7	0.94	0.41	26.1	511	58	3.6	1.2
					596	59		

To overcome the low branching ratio or the excess dose bring by additional particles, improvement has to be made concerning the overall PET detection efficiency to reduce the injected activity to the patient. The use of time-of-flight PET to improve the signal-to-noise ratio is one possibility while using 3-gammas imaging is another one.

Several radiometals present a prompt gamma ray emission accompanying the positron emission (^{34m}Cl , ^{44m}Sc , ^{52}Mn , ^{86}Y , ^{94}Tc , ^{152}Tb). This additional emission is often considered as an increase of the radiation burden to the patient. However dedicated camera are under development to measure in the same time the line of response generated by the annihilation and the third photons.^{5,6,7,8,9} The intersection of the two lines will decrease the uncertainty on the annihilation position and then lead to a signal to noise increase and a decrease of the overall patient exposure.

The fact that there are two major radionuclides of copper that are of interest for theranostic applications is another important factor to push forward ^{64}Cu as a PET radiometal candidate. The therapy based on diagnostics is one way to achieve personalized medicine. A “control” image can be obtained prior to inject the selective therapeutic molecule to the patient. A PET (or SPECT) isotope is coupled to the molecule of interest and injected to the patient. The tumor and healthy tissues uptake can be visualized and the concentration of the molecule can be quantified and used to individually adapt the therapeutic dose delivered to each patient. In order to have the same *in vivo* behavior between the molecule used for the dosimetry image and the one used for the therapeutic dose, radioisotopes of the same element should be used to ensure identical biochemical behavior. There is “matched pairs” of several elements that can be of interest for theranostic approach: iodine (123, 124, 125, 131), Yttrium (86, 90), Copper (61, 62, 64, 67), Lead (203, 212), Terbium (149, 152, 155, 161) and Arsenic (71, 72, 74, 77)

B.2 Production of isotopes

The main nuclear reactions involved to produce radioisotopes are neutron capture, fission and induced reactions using proton or light ion. The two main installations where those nuclear reactions can occur are nuclear reactor and accelerator facilities. Reactor provides a high flux of neutrons while cyclotrons and linear accelerators increase the energy of protons or light ions before reaching the target of interest.

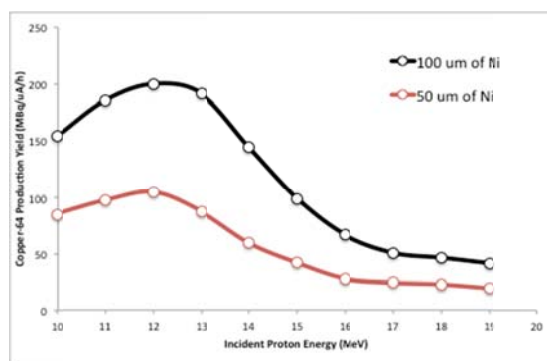
Whatever the production method, the main properties required to produce radioisotopes for medical applications are the capability to produce a large amount of activity, the specific activity and the radioisotopic purity of the solution. The specific activity can be defined as the ratio between the required isotope and others isotopes of the same element present in the mixture. The radioisotopic purity highlights the amount of unwanted radioisotopes in the solution.

Copper-64 can be produced either by research reactor or accelerator. The reactor solution involves a radiative (n, γ) reaction with a relatively high specific activity. A high purity enriched ^{63}Cu target is used (*i.e.* 63.9 % natural abundance). The calculated production yield of ^{64}Cu by neutron irradiation of enriched ^{63}Cu reaches 3.7 GBq/mg when the target is irradiated 40 hours with a thermal neutron flux of $10^{14} \text{ n.s}^{-1}.\text{cm}^{-2}$ and goes up to 30 GBq/mg when the neutron flux grows by one order of magnitude (IAEA, technical report 1340).

Nowadays, the most common production method utilizes $^{64}\text{Ni}(p,n)^{64}\text{Cu}$ reaction. Szelecsenyi *et al* were the first to propose this reaction on a biomedical cyclotron.¹⁰ The enriched ^{64}Ni target (99.6 %, few mg) is prepared and electroplated onto a gold disk.

Figure 1 shows the calculated production yield for two target thicknesses. With an energy of 12 MeV, 100 MBq/ μAh can be reached with a 50 μm ^{64}Ni target. As an example, Obata *et al* reported an average yield of 70 MBq/ μAh .¹¹ The $^{64}\text{Ni}(d,2n)^{64}\text{Cu}$ reaction can also be used. Daraban *et al* published a production yield of 844 MBq/ μAh in the 20.5-9 MeV region.¹²

Figure 1: Copper-64 production yield using the $^{64}\text{Ni}(p,n)^{64}\text{Cu}$ reaction

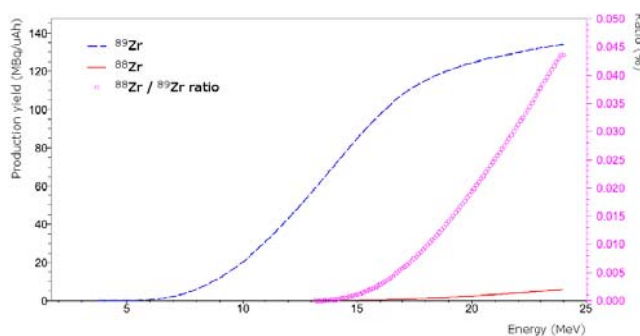


As a comparison, the production yield at saturation for the $^{18}\text{O}(p,n)^{18}\text{F}$ reaction on a liquid target is around 14 GBq/ μA (IAEA, technical report 468). This non-exhaustive description of ^{64}Cu production demonstrates that a reasonable yield can be achieved on a biomedical cyclotron. However, it has to be noted that enriched ^{64}Ni is expensive due to its low natural abundance (0.95 %) and directly affect the overall price. Recycling of the target is then necessary to obtain reasonable cost. A recent review regarding the copper radioisotopes can be found in Asabella *et al*¹³ and a review on ^{64}Cu for PET imaging can be found in Anderson *et al*.¹⁴

Generator-produced radionuclides are attractive for use in biomedical applications and seem to be an ideal solution for clinical settings. ^{68}Ga can be produced by a (p,n) reaction on ^{68}Zn but it is usually eluted from generators. Gleason first described the $^{68}\text{Ge}/^{68}\text{Ga}$ generator in 1960.¹⁵ ^{68}Ge can be produced in an accelerator facility using a variety of charged particle induced nuclear reactions. ^{68}Ge then decays via electron capture to ^{68}Ga with a half-life of 270.95 days. In order to estimate which nuclear reaction is the most productive to obtain ^{68}Ge , a lot of efforts have been devoted to measure the different excitation functions. From the literature, it seems that nuclear reactions on gallium targets offer a production with no-carrier-added ^{68}Ge . The maximum cross section for both the ^{69}Ga and ^{nat}Ga targets is obtained for proton energy in the 20 MeV region. A complete description of ^{68}Ge production can be found in the report from IAEA (IAEA, production of long lived parent radionuclides for generators: ^{68}Ge , ^{82}Sr , ^{90}Sr and ^{188}W). Two important aspects have to be highlighted: *i*) due to the long half-life of ^{68}Ge , high current cyclotrons with beam intensity higher than 100 μA are required to reach a sufficient production yield. In addition, long-term irradiation periods of several days are mandatory. Only few facilities can handle all this difficulties. *ii*) The mechanical and chemical design of the targets are crucial issues and have to take in consideration the thermal aspect of high current irradiations, the corrosion and radiation resistance.

^{89}Zr can be produced in an accelerator facility using ^{89}Y solid target (100 % natural abundance). Two nuclear reactions have been investigated in the literature: $^{89}\text{Y}(p,n)^{89}\text{Zr}$ and $^{89}\text{Y}(d,2n)^{89}\text{Zr}$. The first reaction is the most commonly used. Irradiation of the yttrium solid target leads to radionuclides impurities and produces two zirconium isotopes: ^{88}Zr and ^{89}Zr . Figure 2 presents the calculated production yield of those two isotopes on a thick target. We can observe that below 12 MeV, the production of ^{88}Zr becomes negligible. Dabkowski *et al* reported at the international workshop on targetry and target chemistry in 2012 a production yield of 8-9 MBq/ μAh with proton beam energy of 9.8 MeV.¹⁶ A recent review on ^{89}Zr production can be found in Kasbollah *et al*.¹⁷

The long half-life Arsenic-71 radionuclide can be produced by $^{70}\text{Ge}(d,n)^{71}\text{As}$ nuclear reaction¹⁸ and by $\text{Ge}(p,xn)^{71}\text{As}$ processes.¹⁹ It has been reported that using this last nuclear reaction, ^{71}As is not producible without contamination. Spahn *et al* reported a production yield of 118 MBq/ μAh for a proton beam over the energy range of 50 to 18 MeV but with a high level of radionuclides impurities (73% of ^{72}As , 5% of ^{73}As and 6.1% of ^{74}As).²⁰ All the production routes share the radiochemical separation of arsenic radionuclides from macroscopic germanium targets.²¹

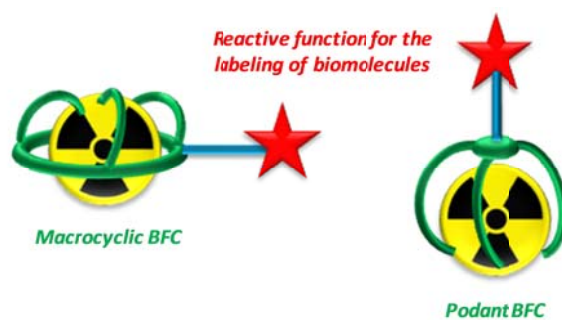
Figure 2: Zirconium 88,89 production yields using the $^{89}\text{Y}(p,n)^{89}\text{Zr}$ nuclear reaction

From the physical properties of the radionuclides and the way they are produced, we can summarize that the radionuclide generator $^{68}\text{Ge}/^{68}\text{Ga}$ system may contribute to PET imaging much as $^{99}\text{Mo}/^{99\text{m}}\text{Tc}$ is doing for SPECT imaging. To target macromolecules requiring longer half-life, ^{64}Cu seems to present appropriate conditions. ^{71}As present interesting physical properties compared to ^{89}Zr when half-lives of few days are required. However the radionuclide impurities level obtained with the proposed production process seems to be a major obstacle for the use of this isotope.

C Availability of bifunctional chelates for Copper, Gallium and Zirconium

Immuno-PET and immuno-radiotherapy rely on the radiolabeling of an antibody of interest. While non-metallic radionuclide such as ^{11}C , ^{13}N , ^{15}O and ^{18}F are typically introduced on biological vectors by the formation of chemical bonds, metallic isotopes need to be sequestered into a bifunctional chelate (BFC). This BFC insures the stability of the complex in the body and provides a reactive function to be covalently couple to the biomolecule of interest. Two classes of BFCs are being developed in order to provide: *i*) fast complexation of the radiometal under high dilution conditions and at room temperature, *ii*) a strong association in a broad range of pH (pH = 1 to 8) and *iii*) a good inertness towards *in vivo* transmetallation by endogenous metal ions (Ca^{2+} or Zn^{2+} for example)²² and transchelation reactions by endogenous ligands, such as transferrin,^{23,24} superoxide dismutase²⁵ and ceruloplasmin.²⁶ The choice of the right chelator is a crucial point in the stability of the radioconjugate and loss or dissociation of the radionuclide results in toxicity and poor image quality.

A large number of ligands have been developed in order to satisfy to the specific requirements of the radiometals in terms of donor atoms, coordination number and geometries and can be classified into two major families: macrocycles and podants (Figure 3).

Figure 3: Two classes of bifunctional chelates (BFCs): macrocycles and podants

Cyclic (Figure 4) and acyclic polyamine ligands (Figure 5) substituted by carboxylate and phosphonate donors are widely used for the complexation of metal cations, including Ga(III), Cu(II) and Zr(IV).²⁷ Acyclic chelators usually provide fast complexation kinetic of the radiometals but are generally less kinetically inert than macrocyclic complexes.

Figure 4: Selected acyclic chelators.

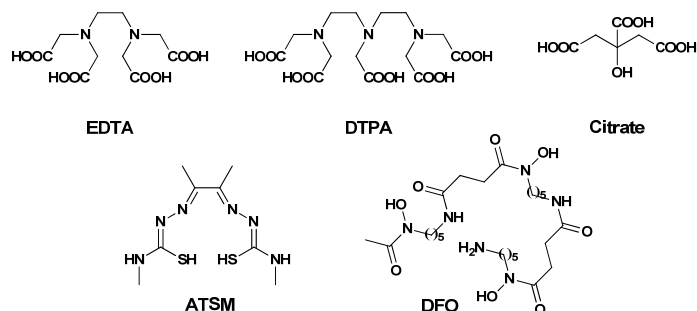
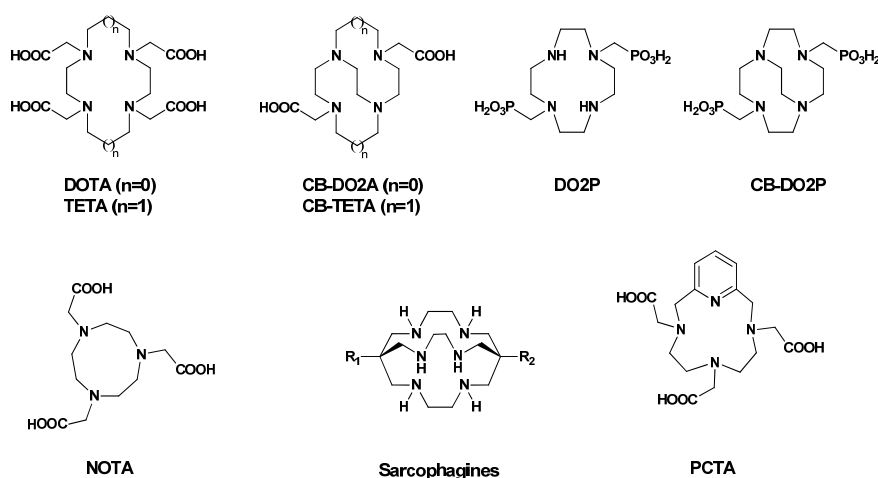


Figure 5: Selected macrocyclic chelators.



EDTA (ethylenediaminetetraacetic acid) is probably one of the oldest synthetic ligand. Originally synthesized by R. Fick and H. Ulrich in 1936, it has been widely used for the complexation of transition metals and displays fast complexation kinetics at room temperature.²⁸ However, serum stability measurements on the ⁶⁷Cu complex revealed that it is not stable in human serum.²⁹ DTPA (diethylenetriaminepentaacetic acid, Figure 4) is another cheap and convenient ligand since it can be obtained in one step from sodium chloromethylacetate and diethylenetriamine.³⁰ Its coordination properties were first studied with Fe(III) in 1968³¹ and DTPA has been found to outperform EDTA.³² Since then, it has been used to coordinate almost all metals of the periodic table, from transition metals to rare-earth elements. It was first used for the synthesis of Technetium-99-DTPA-protein complexes for scintigraphy in 1981.³³

As seen from the number of publications over the past twenty-five years (Figure 6), DOTA (1,4,7,10-tetraazacyclododecane-1,4,7,10)-tetraacetic acid, Figure 5) is the most popular macrocyclic chelator for the complexation of radiometals. Its complexation properties were first studied by H. Stetter and W. Frank in 1976, showing outstanding complexation of alkaline earth metals (Ca, in particular) as well as strong binding of transition metal ions such as Cu, Ni, Co, Zn, Cd and for Pb.³⁴ One year later, J. F. Desreux demonstrated that DOTA could also form very stable lanthanide complexes in water (La, Eu, Pr and Y).³⁵ Moreover, it forms overall more stable complexes than DTPA and was for a long time considered as a universal ligand for imaging applications such as MRI, PET, SPECT and fluorescence imaging.³⁶ In particular, [Gd(DOTA)]⁻ has been used as a clinical MRI contrast agent since the 90's (DOTAREM[®], Guerbet).

The last five years are characterized by a decline in the use of DOTA for radiolabeling applications together with a growing number of alternative ligands (Figure 6). The development of new bifunctional chelates for the coordination of radiometals is far from being a futile task, since it has now become clear that, due to the large diversity in the properties of the radiometals and their differing coordination chemistries, there cannot be a universal chelate suitable for all radionuclide. Larger tetraazamacrocycles such as TETA (TETA = 1,4,8,11-tetraazacyclotetradecane-1,4,8,11-tetraacetic acid) have been developed in order to provide 6-membered chelate rings.³⁷ Triazacyclononane derivatives (NOTA = 1,4,7-triazacyclononane-1,4,7-triacetic acid) provide a smaller coordination pocket with a restricted number of binding

atoms. Investigations have been performed on reinforced systems, namely, cross-bridged and side-bridged chelates, with the aim to increase kinetic inertness of the Cu(II) complexes. This review is aimed to provide general notions about the coordination chemistry of Ga(III), Cu(II) and Zr(IV), when designing a PET imaging agent. It seemed neither realistic nor appropriate for us to endeavour to present a comprehensive review of the ligands developed within the last 30 years or so. For more detailed information, interested readers are referred to recent excellent review articles on this topic.^{3,38,39,40}

Figure 6: Left: Number of publications using classical macrocyclic ligands (DOTA, NOTA, TETA, ATSM, CB-DO2A, CB-TE2A, DO2P, CB-DO2P, Sarcophagines, PCTA), podants (EDTA, DTPA, DFO) and their derivatives used for radiolabelling applications; Right: Evolution of the relative percentage of the different ligands.

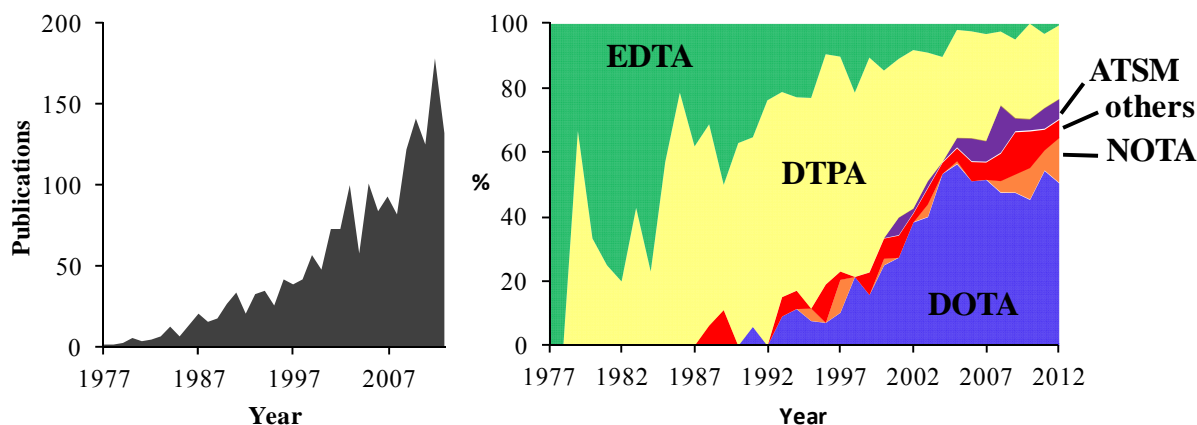


Table 2: Thermodynamic stability constants, redox potentials (*q-rev* = quasi-réversible, *irrev* = irreversible) and kinetic inertness towards acid-assisted dissociation of selected Ga(III) and Cu(II) complexes.^{38,3,41,39}

	M	Log K _{ML}	E _{red} vs NHE	t _{1/2}
Macrocyclic chelators				
DOTA	Ga	21.3		
	Cu	22.2, 22.7	-0.74 (<i>irrev</i>)	<3 min (5M HCl, 90°)
NOTA	Ga	31.0		
	Cu	19.8, 21.6	-0.70 (<i>irrev</i>)	<3 min (5M HCl, 30°)
TETA	Ga	19.7		
	Cu	21.1, 21.9	-0.98 (<i>irrev</i>)	<3 min (5M HCl, 90°)
CB-DO2A	Ga			
	Cu		-0.79 (<i>irrev</i>)	4.0 h (1 M HCl, 30°)
CB-TE2A	Ga			
	Cu		-0.88 (<i>q-rev</i>)	154 h (5M HCl, 90°)
DO2P	Ga			
	Cu	28.7		
DiamSar	Ga			
	Cu		-0.90 (<i>irrev</i>)	40h (5M HCl, 90°)
PCTA	Ga			
	Cu	19.1		
Acyclic chelators				
EDTA	Ga	18.8, 19.2		
	Cu	21.0, 22.0		
	Zr	27.7, 29.4		
DTPA	Ga	25.5		
	Cu	21.4		
ATSM	Zr	35.8, 36.9		
	Ga			
DFO	Cu		-0.40 (<i>q-rev</i>)	
	Ga	28.6		
	Cu	19.2		

C.1 Chelates for Ga-68

Gallium is a post-transition metal of electronic configuration $[\text{Ar}]3d^{10}4s^24p^1$. Its chemistry in aqueous solution is exclusively limited to the +3 oxidation, which has a diamagnetic d^{10} configuration and a small ionic radius of 47-62 pm for coordination numbers of 4 to 6.⁴² As a classic hard acidic cation, it is strongly bonded to hard donor ligands featuring multiple nitrogens and anionic oxygens such as carboxylate, phosphonate or phosphinate functions. Two points need to require specific attention when designing Ga(III)-based radiopharmaceuticals: (i) their resistance to hydrolysis and (ii) to transchelation reactions, which occur in particular with transferrin, due to the strong competition between Ga(III) and Fe(III).²³ At physiological pH, gallium displays a strong affinity for hydroxide ions and forms insoluble $[\text{Ga}(\text{OH})_3]$,⁴³ whereas free hydrated $[\text{Ga}(\text{H}_2\text{O})_6]^{3+}$ is stable only under acidic conditions ($\text{pK}_a = 2.6$).⁴⁴

67-Gallium citrate is used as a γ emitter for SPECT since the mid 70's. Citrate is a weak Ga(III) chelator and is known to give transchelation reactions with transferrin, lactoferrin and ferritin *in vivo*,⁴⁵ which leads to an accumulation of the Ga-67 in the lungs immediately after intravenous injection. Because of its low specificity and significantly high radiotoxicity, it is only used where and when ^{18}F -FDG PET is not available. However, $[\text{Ga}(\text{citrate})\text{OH}]^-$ ($\log \beta_{\text{MLOH}} = 7.1$)⁴⁶ can be used as a pre-complexing agent for the synthesis of Ga(III) complexes of higher stability.⁴⁷ For instance, thermodynamically stable and kinetically inert Ga(III) complexes have been obtained by sequestering Ga(III) with hexadentate ligands (Table 2).^{38,3} DOTA analogues have mainly been used and the ^{68}Ga complexes have been tested pre-clinically for the targeting of somatostatin,⁴⁸ bombesin^{49,50} and melanocortin 1 receptors.⁵¹ ^{68}Ga -DOTA conjugates with octreotide (^{68}Ga -DOTATOC), and analogue peptides (^{68}Ga -DOTATATE and ^{68}Ga -DOTANOC) are currently in clinical trials for diagnosing somatostatin-receptor positive tumours.⁵² NOTA is known to form very stable Ga(III) complexes (Table 2).⁵³ Its C-functionalised derivative (NODAGA) is becoming increasingly more popular since it outperforms most of the other DOTA analogues, especially with regard to facile radiolabeling (30 to 60 minutes at ambient temperature).^{54,50}

Among the recent advances, triazacyclononane-triphosphinate derivatives (TRAP, $\log K_{\text{ML}} = 26.24$, NOPO⁵⁵) have been developed with the aim to increase Ga(III) selectivity and *in vivo* stability. A N_4O_2 linear chelating agent (H_2dedpa , Figure 7)⁵⁶ and its nitroimidazole derivative⁵⁷ show very good radiolabeling efficiencies in mild conditions as well as exceptional kinetic inertness *in vitro*. Bis-phosphonate conjugates have also been studied for bone imaging⁵⁸ and $[\text{Ga}[\text{NO}_2\text{A}-\text{N}-(\alpha\text{-amino})\text{propionate}]]$ for *in vivo* pH sensing.⁵⁹

C.2 Chelates for Cu-64

Copper is a first row transition metal of electronic configuration $[\text{Ar}]3d^{10}4s^1$. It displays three oxidation states in aqueous solutions, Cu(I-III). Cu(I) has a diamagnetic d^{10} configuration and is stabilized by soft ligands such as thioethers, thiolates, phosphines, nitriles, isonitriles, cyanide. Cu(II) is the most widely used oxidation state for radiopharmaceuticals. It is paramagnetic and stands on the border between hard and soft metals. As a consequence, it has a strong affinity for ligands containing nitrogen donors but also hard anionic oxygens or soft sulfur donors. Cu(III), is relatively rare and is only observed when coordinated to strong π -donating ligands.⁶⁰

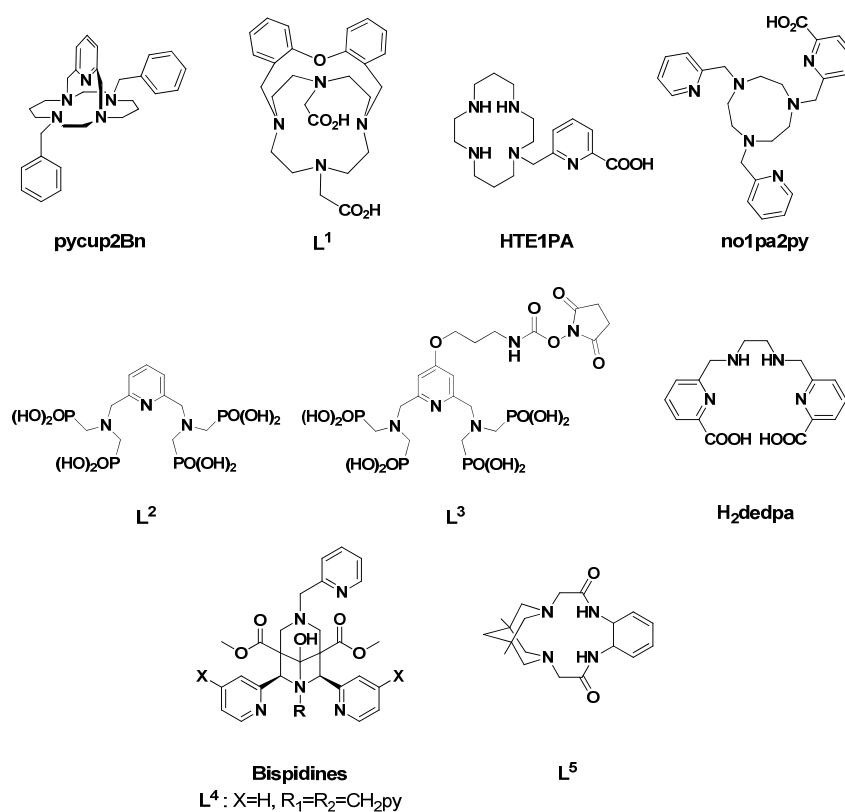
Historically, cyclic and acyclic tetradentate chelators (N_4 , N_2O_2 and N_2S_2) were favored in order to stabilize the d^9 electronic configuration of Cu(II). Cyclam and its derivatives form complexes with high thermodynamic stability⁶¹ although not kinetically inert. Bis(thiosemicarbazonato) ligands such as ATSM (Figure 4) coordinate as a tetradentate chelate in a planar arrangement. The complexes are characterized by a very low redox potential (Table 2) and $[\text{Cu}(\text{ATSM})]$ is spontaneously reduced when entering a cell and reoxidized by molecular oxygen in a reversible process.⁶² $^{64}\text{Cu}(\text{ATSM})$ has been used very effectively for the detection of hypoxic tumor cells and is currently in clinical trials.⁶³

Stable complexes with coordination numbers of 5 and 6, with trigonal bipyramidal and distorted octahedral geometries (due to Jahn-Teller distortions) have now become the most investigated in radiocopper chemistry since they provide a better envelopment of the Cu(II) ion and tend to be more kinetically inert. So far, a wide range of polyazaamacrocyclic ligands, based on cyclen, cyclam and triazacyclononane backbones, have been studied.^{39,64,65} Although they have been extensively used as chelators for ^{64}Cu -labeling of peptides, DOTA and TETA are not ideal chelators for Cu(II) and *in vivo* experiments in rat models have shown that both complexes undergo transchelation of $^{64}\text{Cu}(\text{II})$ to liver and blood proteins.⁶⁶ NOTA is now emerging as the best alternative to DOTA since it is commercially available and can be used for the labeling with ^{64}Cu with very high specific activity and under mild reaction conditions (30-60 min at room temperature).⁶⁷ Moreover, although the stability constant of $[\text{Cu}(\text{NOTA})]^-$ is very similar to the ones of $[\text{Cu}(\text{DOTA})]^{2-}$ and $[\text{Cu}(\text{TETA})]^{2-}$ (Table 2), it displays a higher *in vivo* stability.³⁹ Metabolic studies in rat models showed that cross-bridged $^{64}\text{Cu}(\text{CB-DO2A})$ and $^{64}\text{Cu}(\text{CB-TE2A})$ (Figure 5) present an increased *in vivo* stability compared with $^{64}\text{Cu}(\text{DOTA})^{2-}$ and $^{64}\text{Cu}(\text{TETA})^{2-}$ complexes, confirming that the introduction of the ethylenic bridge enhances the stability of these macrocyclic complexes.^{68,69} CB-TE2A also possesses the capacity to stabilize Cu(I) and is practically inert towards Cu(II)/Cu(I) reduction ($E_{\text{red}} = -0.88$ V). However, these constraints significantly slow down the kinetics of Cu(II) complexation and renders difficult the labeling of heat-sensitive biomolecules such as antibodies.⁷⁰ Cross-bridged cyclam and cyclen macrocycles having methanephosphonic acid pendant arms, CB-DO2P and CB-DO2P (Figure 5), have been developed^{71,72} and the corresponding ^{64}Cu complexes demonstrated promising kinetic inertness *in vivo*. Side-bridged cyclam derivatives are also strong candidates since they allow for quantitative radiolabeling with ^{64}Cu in EtOH and *in vitro* stability in human serum.⁷³ Hexaaminemacrobicyclic type structures such as sarcophagines^{74,75,76,77} form hexacoordinated and octahedral Cu(II) complexes at room and negligible *in vitro* transchelation was observed. Despite their very promising properties, the application of sarcophagine derivatives has until

now been limited by their long and tedious synthetic pathway. This barrier has recently been challenged by E. Mume *et al.*, who developed a high yielding synthesis method.⁷⁸

Two new cyclam (pypcup2Bn)⁷⁹ and cyclen (**L**¹)⁸⁰ cross-bridged macrocycles (Figure 5) form stable complexes with Cu(II) ($\log K_{\text{CuL}} = 23.25$ for **L**¹) and demonstrate very good kinetic inertness towards acid-assisted dissociation ($t_{1/2} = 20.3$ h in 5M HCl 90°C for Cu-pypcup2Bn and $t_{1/2} = 30.8$ d in 12M HCl 90°C for **L**¹). For both systems, complexation kinetic is slow at room temperature. Nevertheless, in the case of pypcup derivatives, quantitative radiolabeling was achieved after 30 min at 60°C. Acyclic ligands based on a pyridine backbone and functionalized by aminomethylphosphonate functions also show great promises for ⁶⁴Cu PET imaging. These ligands display a very strong complexation toward Cu(II) ($\log K_{\text{CuL}} = 22.7$ for **L**²), combined to a high selectivity for Cu(II) towards Ni(II), Co(II), Zn(II) and Ga(III) ($\Delta\log K > 4$).^{81,82} **L**² can be derivatized into an activated phosphonated bifunctional chelate **L**³ (Figure 7), which can be coupled to small peptides or large antibodies.⁸³ Several other ligands based on picolinate units such as dedpa ($\log K_{\text{CuL}} = 19.2$)⁸⁴, HTE1PA ($\log K_{\text{CuL}} = 25.5$ and $t_{1/2} = 32$ min in 1M HCl 25°C),⁸⁵ no1pa2py ($\log K_{\text{CuL}} = 21.0$)⁸⁶ have recently been reported and exhibit high selectivity and fast complexation kinetics (Figure 7). Metabolism study of [⁶⁴Cu(TE1PA)]⁺ assessed a good *in vivo* stability.⁸⁷

Figure 7: Emerging families of ligands for Ga-68 and/or Cu-64 complexation.



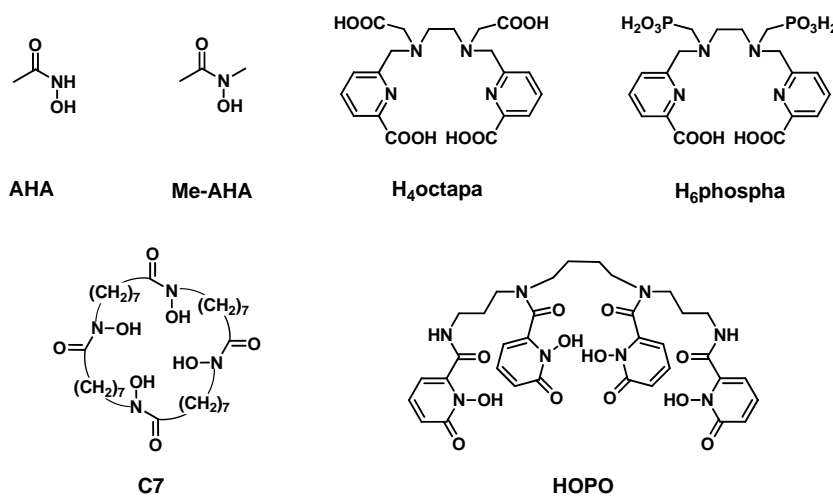
Pyridyl substituted bispidine (3,7-diazabicyclo[3.3.1]nonane) ligands⁸⁸ and bispidine fused with dioxotetraaza macrocycles (**L**⁵, Figure 7)⁸⁹ are also strong candidates for the complexation of ⁶⁴Cu, as shown by ⁶⁴Cu transchelation tests in SOD and in human serum at 37°C. Biodistribution studies of ligand **L**⁴ in rats models have shown a very rapid blood and normal-tissue clearance for most organs and tissues.⁹⁰ 2,4-pyridyl-substituted bispidine have the advantage to be readily obtained in few synthetic steps.⁹¹

C.3 Chelates for Zr-89

Zirconium is another transition metal ($[\text{Kr}]4d^25s^2$). In aqueous solution, it is present under its +4 oxidation state, with a small ionic radius (59-89 pm for CN 4-9). As a consequence, Zr(IV) is extremely hard and its chemistry is dominated by hydrolysis and poly oxo/hydroxo species.⁹² Polyanionic ligands such as EDTA,⁹³ DTPA⁹⁴ and DOTA⁹⁵ form eight-coordinated complexes with Zr(IV) with strong affinity (Table 2).^{95,96,97,98} However, the complexes display poor *in vivo* stability.⁹⁹ Desferrioxamine (DFO, Figure 4) is from far the most used ligand for the synthesis of Zr-based radioconjugates. Since the first clinical studies in 2006,^{100,101} a large number of ⁸⁹Zr-DFO-antibody conjugates are in clinical trials for various applications^{102,103} such as metastatic prostate cancer,^{104,105} breast cancer,¹⁰⁶ and for the detection of sentinel lymph nodes.¹⁰⁷ However, upon time, ⁸⁹Zr is released and small accumulation in bones is observed.^{108,109} Several groups have now

undertaken the study of the aqueous chemistry of Zr(IV) with DFO and, more generally, hydroxamates such as acetohydroxamic acid (AHA) and N-methyl-acetohydroxamic acid (Me-AHA),¹¹⁰ with the aim to design improved chelators. In particular, a recent DFT study of the mechanism and reactivity of Zr(IV) with Me-AHA confirms that hydroxamate ligands with increased denticity (8 instead of 6 in the case of DFO) will provide complexes with increased thermodynamic and kinetic stability.¹¹¹ As a consequence, a series of macrocyclic ligands, incorporating four hydroxamate units has been synthesized. These ligands demonstrated excellent complexation abilities (Figure 8) and the complexes display strong kinetic inertness. Moreover, improved stabilities compared with the reference DFO have been predicted from quantum chemical studies, which opens bright perspectives for these new ligands. Other coordination units have also been studied. Methyl carboxylate (H₄octapa) and methylphosphonate derivatives of H₂dedpa (H₆phospa) have been studied for the complexation of ⁸⁹Zr. Improvements in ⁸⁹Zr radiolabeling were observed with an advantage for the phosphonated ligand over the carboxylic acid derivatives although the radiolabeling yield remains weak (12% at 37°C).¹¹² Hydroxypyridinone (HOPO) derivatives appear as a good alternative to DFO since they can be radiolabelled in almost quantitative yields (>98% with high specific activity) at millimolar concentration by using the standard procedure used for the complexation of DFO, *ie.* by addition of ⁸⁹Zr-oxalate at room temperature and pH 6 to 7.¹¹³ However, recent studies have demonstrated a significant loss of affinity upon bio-conjugation. For instance, the ⁸⁹Zr-CP256-trastuzumab immunoconjugate was shown to be less stable *in vivo* than ⁸⁹Zr-HOPO-trastuzumab and a strong uptake in bones and joints was observed.¹¹⁴

Figure 8: Other ligands for Zr-89 complexation.

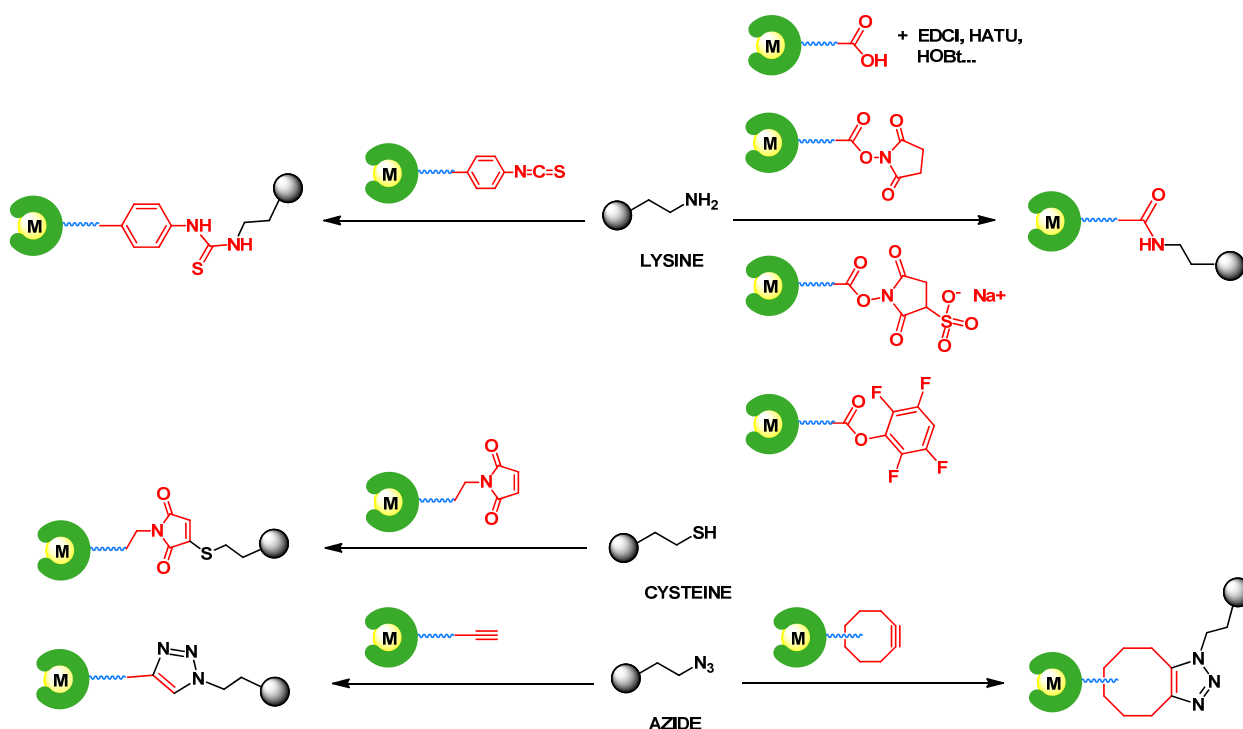


C.4. Principle reactive functions and conjugation strategies

The simplest conjugation strategy, which has long been used in the field, takes advantage of one of the acetate pendant arms, which is involved in amide bond formation with primary amines from lysine residues. However, the transformation of one of the carboxylic acid group into a carboxamide has a strong influence on metal binding properties and decreases *in vitro* and *in vivo* stabilities of the resulting complexes.¹¹⁵ Well-established methods of selective N- and C-functionalization have been developed in order to enable the coupling with the biomolecule without compromising the stability of the respective metal complexes.¹¹⁶ Functionalization is found either on the coordinating pendant arm,^{117,118,119} or on the methylenic backbone of the chelator, which is more elegant and also avoids the multistep synthesis of a sophisticated pendant arm.^{64,120,121,122} Once the bifunctional chelate synthesized, its use as radiopharmaceuticals will still strongly depend on *i)* the effectiveness of the bio-labelling reaction on a accessible function of the target biomaterial (peptide, protein or antibody) which does not perturb the biological activity, *ii)* its ease of implementation in bio-friendly conditions (usually in aqueous buffered media at pH close to neutrality or slightly basic, and at temperatures ranging from 4 to 40°C) and *iii)* the pharmacokinetic and biodistribution of the radiometallated bioconjugate. Most popular activated functions are targeted towards lateral functions of amino acids, either the amine of lysine or the thiol found in cysteine.¹²³ A guide to the construction of ⁶⁸Ga, ⁶⁴Cu and ⁸⁹Zr labelled peptide-, antibody- and oligonucleotide-bioconjugates has been published by B. M. Zeglis and J. S. Lewis.⁶⁴ Additional information can also be found in more recent reviews.^{40,116,124} Activated carboxylic acid with succinimydyl ester (NHS),^{125,83} isothiocyanate,^{126,127,128} N-hydroxysulfosuccinimydyl ester (SNHS),¹²⁹ tetrafluorophenol (TFP)¹³⁰ or peptide coupling reagents such are EDCI, HATU, HOBt... can easily react with primary amines to form a stable peptidic bond (Figure 9). BFCs functionalized with maleimide units are used to regioselectively target thiol functions with quantitative coupling yields.^{131,132} Click-chemistry reactions are attracting a growing interest in the radiopharmaceutical community.¹³³ The copper-catalyzed 1,3-dipolar Huisgen cycloaddition between terminal alkynes and azide is an extremely efficient reaction.¹³⁴ However, the requirement of a toxic Cu(I) catalyst has prevented its application in living systems. Copper-free alternatives based on the use of highly

strained cyclooctyne derivatives have now been used for labeling reactions *in vitro*¹³⁵ and in living organisms.¹³⁶ Additionally, the spacer that separates the chelating moiety and the bioactive fragment can be used as pharmacokinetic modifiers. For instance, a polyethyleneglycol (PEG) chain will increase water solubility, whereas an aliphatic chain will increase lipophilicity.

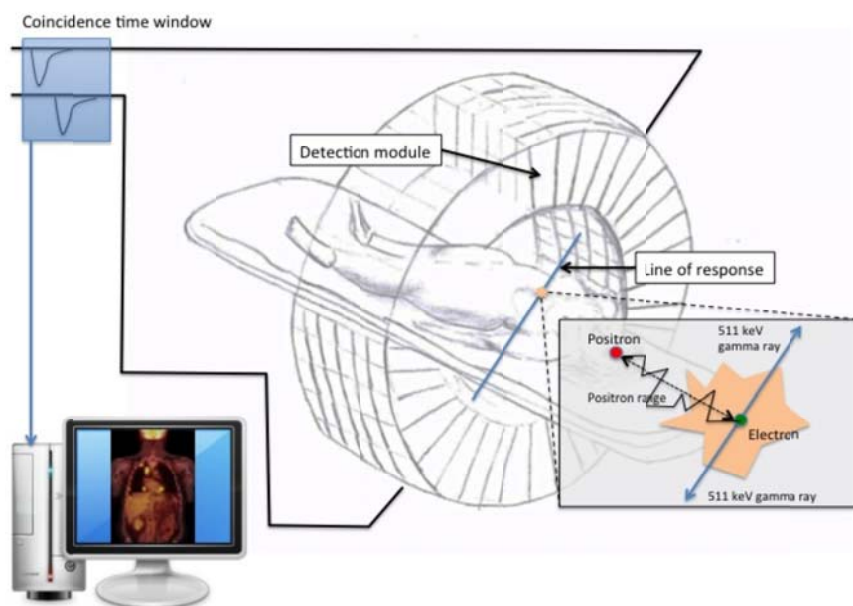
Figure 9: Main activated functions used for bioconjugation of radiotracers towards lysine and cysteine amino-acids.



D Improvement in PET signal-to-noise ratio

Nowadays, a typical commercial clinical PET scanner is made of multi-full-ring detector modules composed of a few ten thousand small scintillation crystals coupled to photodetectors to detect the two 511 keV photons emitted by the radiotracers in the patient body (Figure 10). Because of the cylindrical nature of the detector arrangement, two opposite photons can be detected almost simultaneously. This event is called coincidence and defined a straight line or line-of-response (LOR). The time window to validate the coincident event is about half a billionth of a second with a coincidence data rate of a million events per second. The absolute detection efficiency (in %) or the sensitivity (in cps/MBq) of a PET scanner is defined as the ratio between the number of recorded coincident events and the number of coincident events emitted by the source. This figure of merit is governed by the solid angle defined by the scanner geometry and the material used to detect the 511 keV photons.¹³⁷ In practice, the geometry of the PET system is mostly defined by the patient size for the scanner bore and the overall cost of the system for the axial extent of the scanner. The whole-body biodistribution of [¹⁸F]-FDG tracer can be obtained in less than 15 minutes.

Figure 10: Schematic representation of PET acquisition.



The challenge of the reconstruction algorithm is to retrieve for each LOR the position where the annihilation occurred. Images with a spatial resolution of about 4 mm are reconstructed with sophisticated algorithms integrating attenuation, normalization and scatter corrections. Today, all PET systems are combined with a CT scanner bringing anatomical information and quick, easy and accurate determination of the attenuation correction required for quantitative imaging.

Improving the signal-to-noise ratio would allow to reduce the patient injected activity and compensate the effect of certain radiometal with low branching ratio, for instance ^{64}Cu .

Initially, PET scanner designs were mainly based on circular arrays of individual crystals leading to a single reconstructed transaxial slice. To improve the axial coverage of the imaging systems, multi-slices or multi-rings systems were introduced with the capability to acquire data in 3D mode. The sensitivity of PET system was further improved by collecting additional coincident events due to the 3D acquisition mode.

An additional step towards a signal-to-noise improvement was done with the introduction of Time-of-Flight (TOF) PET. A variance reduction in the reconstructed data can be obtained by incorporating the TOF information in the reconstruction procedure. The idea to use the time information in the reconstruction procedure was originally proposed in the 1960's but the first systems were only built twenty years after. The concept of TOF PET is to calculate for each coincident event the time difference between the arrival of each 511 keV photon defining the LOR. This time information helps to localize the annihilation position on the LOR. When TOF acquisition is not applied, the data collected on each LOR is backproject through a distance defined by the intersection of the LOR with the patient. With TOF information the same data are only backproject through a smaller distance equivalent to the uncertainty window of the annihilation-estimated position. The gain in sensitivity due to TOF PET can be approximated by the ratio between the diameter of the object and the space window defined by the timing resolution of the system.

The first TOF PET systems were built with cesium fluoride or barium fluoride crystals leading to a system coincidence timing resolution around 700 ps. Nowadays with the introduction of new fast crystals, coincidence timing resolution below 200 ps have been obtained.^{138, 139, 140} Gundacker *et al* mentioned in their article that a coincidence timing resolution of 100 ps corresponds to an annihilation position resolution on the LOR of 1.5 cm leading to a signal-to-noise gain of 5. Although the relation between the signal-to-noise ratio, the injected activity and the image quality is not evident and linear, we can observe that the use of TOF PET can already minimize the effect of ^{64}Cu low branching ratio.

The PET detection efficiency depends also on the solid angle of the scanner and the detector material used to convert the 511 keV annihilation photons to lower energy optical photons.

The solid angle of the scanner is mainly determined by the diameter and the axial extent of the system. A modification on these parameters directly impacts the overall system price. Another solution is to use thicker crystal element to improve the detection efficiency. As an

example, 8 mm of LSO:Ce crystal are required to attenuate 50 % of 511 keV. In order to collect 90% of impinging 511 keV photons, 25 mm of crystal are needed which lead to 81% detection efficiency in coincidence mode. Unfortunately, the uncertainty on the scintillation position increases with the thickness of the crystal. The trade-off is a reduction in spatial resolution through parallax errors due to the lack of accurate measurement of the depth of interaction (DOI). Two or more crystal layers can be used to sample the depth and then obtain an estimation of the DOI.¹⁴¹ Moses *et al* was the first to measure the DOI using an additional array of photodiodes in the front side of the block detector.¹⁴² Several groups after have used the same concept with an LSO scintillator array coupled at both sides by semiconductor photodetectors.^{143,144,145} Contrary to the phoswich method, this method allows a continuous sampling of the DOI. However, in the 1970s, Ter-Pogossian *et al* pioneered an original concept where the NaI crystals were positioned according to the axial direction with a PMT at each end of the crystal.¹⁴⁶ The principle advantage of this geometry is that, due to a simplification in the depth encoding procedure, neither resolution nor sensitivity is compromised. The crystal section gives the transverse spatial resolution and the light sharing between both photodetectors gives the spatial resolution in the axial direction. The detection efficiency depends on the number of crystals in the radial direction. Several groups have been investigated this geometrical approach.^{147,148,149} In Salvador *et al*, a spatial resolution in the axial direction of 1 mm FWHM has been achieved with LYSO:Ce crystal of 1.5 x 1.5 x 25 mm³.^{150,151}

Casabella *et al* recently published a high resolution TOF PET concept with axial geometry. A coincidence timing resolution of 211 ps (FWHM) is reported constraining the annihilation point on the LOR to 3.1 cm (FWHM).¹⁵²

Conclusion

In 1964, Hacket *et al*¹⁵³ published 4 compounds as promising agents for use with ⁶⁴Cu in the localization of brain tumors: alanine, cysteine, isonicotinic acid hydrazide and DTPA. Fifty years later, all these compounds have been proven to suffer from low *in vivo* stability. More than twenty Cu(II) chelates have been synthesized and tested in order to provide a strong coordination pocket and to avoid the release of Cu(II) in the body. These compounds have been linked to antibodies, proteins, peptides and nanomolecules for preclinical and clinical researches. At the same time, ⁶⁴Cu-ATSM, which uptake mechanism is based on Cu(II) reduction followed by decomplexation, is showing great promises for hypoxic tumors and is currently being tested in phase II for cervical cancer in the US. Moreover, in an era of outstanding accomplishments in personalized medicine and theranostic, ⁶⁴Cu and its brother ⁶⁷Cu show great advantages as a dual PET imaging agent and radionuclide for the radioimmunotherapy of tumours. Despite all these efforts, it seems that we still lack of clinical killer applications pushing a ⁶⁴Cu radiolabelled molecule in front of the scene, as none of the ⁶⁴Cu-radioconjugate has been implemented to phase III studies yet.

⁶⁴Cu is not the only radiometal tagged as innovative radionuclide and this paper investigates the critical criteria such as the physical properties, the production capability and the associated molecule to become a success story. As the majority of the actual literature, we highlight 3 radiometal isotopes having the potential for PET imaging: ⁶⁸Ga produced by generator may contribute to PET imaging as ^{99m}Tc is doing for SPECT, ⁶⁴Cu to label macromolecules if the sensitivity of the PET systems is improved and ⁸⁹Zr when longer half-lives are required.

In conclusion, it seems that progresses are being held hostage by the fragility of the financial systems, which makes investors more risk averse than a decade ago. At the moment, all the radiopharmaceutical industry is still focused on FDG production and the cyclotron production sites and the clinical PET facilities are almost saturated making FDG a quasi-inexpensive molecule. It's then difficult to correctly appreciate the industrial and health public authorities' capacities to introduce a new radiolabelled molecule on the market at the level of FDG.

Acknowledgements

We acknowledge CNRS for financial support, as well as Dr Loïc Charbonnière for fruitful discussions and careful reading of this review. We also acknowledge Dr Eric Garrido for the analytical evaluation of ⁶⁴Cu and ^{88,89}Zr production yields.

Notes and references

^a Université de Strasbourg, IPHC, 23 rue du Loess 67037 Strasbourg France

^b Université de Strasbourg, IPHC, 23 rue du Becquerel 67087 Strasbourg France .

^c CNRS, UMR7178, 67087 Strasbourg, France.

- ¹ T. Beyer, D. W. Townsend, T. Brun et al, *J. Nucl. Med.*, 2000, **41**(8), 1369.
- ² G. Muehlethner, J. S. Karp, *Phys. Med. Biol.*, 2006, **51**, R117.
- ³ E. W. Price, C. Orvig, *Chem. Soc. Rev.*, 2014, **43**, 260.
- ⁴ C. S. Cutler, H. M. Hennkens, N. Sisay, S. Huclier-Markai, S.S. Jurisson, *Chem. Rev.*, 2013, **113**, 858.
- ⁵ C. Grignon, J. Barbet, M. Bardie, T. Carlier, J.F. Chatal, O. Couturier, J.P. Cussonneau, A. Faivre, L. Ferrer, S. Girault, T. Haruyama, P. Le Ray, L. Luquin, S. Lupone, V. Métivier, E. Morteau, N. Servagent, D. Thers, *Nucl. Instr. Meth.*, 2007, **571**, 142.
- ⁶ T. Oger, W.-T. Chen, J.-P. Cussonneau, J. Donnard, S. Duval, J. Lamblin, O. Lemaire, A.F. Mohamad Hadi, P. Leray, E. Morteau, L. Scotto Lavina, J.-S. Stutzmann, D. Thers, *Nucl. Instr. Meth.*, 2012, **695**, 125.
- ⁷ J. Donnard, W.-T. Chen, J.-P. Cussonneau, S. Duval, J. Lamblin, O. Lemaire, A. F. Mohamad Hadi, P. Le Ray, E. Morteau, T. Oger, L. Scotto Lavina, J.-S. Stutzmann, D. Thers, *Nucl. Med. Rev.*, 2012, **15**, C64.
- ⁸ T. Kormoll, F. Fiedler, S. Schöne, *Nucl. Instr. Meth. A*, 2011, **626-627**, 114.
- ⁹ F. Roellinghoff, M.-H. Richard, M. Chevallier, J. Constanzo, D. Dauvergne, N. Freud, P. Henriquet, F. Le Foulher, J. M. Létang, G. Montarou, C. Ray, E. Testa, M. Testa, A. H. Walenta, *Nucl. Instr. Meth. A*, 2011, **648**, s20.
- ¹⁰ F. Szelecsenyi, G. Blessing, S. M. Qaim, *Appl. Radiat. Isotopes*, 1993, **44**, 575.
- ¹¹ A. Obata, S. Kasamatsu, D.W. McCarthy, M.J. Welch, H. Saji, Y. Yonekura, Y. Fujibayashi, *Nucl. Med. Biol.*, 2003, **30**, 535.
- ¹² L. Daraban, R. A. Rebeles, A. Hermann, *Appl. Radiat. Isotopes*, 2009, **67**, 506.
- ¹³ A.N. Asabella, G.L. Cascini, C. Altini, D. Paparella, A. Notaristefano, G. Rubini, *BioMed Res. Int.*, 2014, **1**.
- ¹⁴ C.J. Anderson, R. Ferdani, *Cancer Biother Radiopharm.*, 2009, **24**, 379.
- ¹⁵ G.I. Gleason, *Int. J. Appl. Radiat. Isot.*, 1960, **8**, 90.
- ¹⁶ A. M. Dabkowski, K. Probst, C. Marshall, *AIP Conf. Proc.*, 2012, **108**, 1509.
- ¹⁷ A. Kasbollah, P. Eu, S. Cowell, P. Deb, *J. Nucl. Med. Technol.*, 2013, **41**, 35.
- ¹⁸ H. C. Beard, *Ntl. Acad. Sci.*, Washington, 1960.
- ¹⁹ D. Basile, C. Birattari, M. Bonardi, L. Goetz, E. Sabbioni, A. Salomone, *Int. J. Appl. Radiat. Isot.*, 1984, **32**, 403.
- ²⁰ I. Spahn, G. F. Steyn, F. M. Nortier, H. H. Coenen, S. M. Qaim, *Appl. Radiat. Isotopes*, 2007, **65**, 1057.
- ²¹ M. Jenneweina, S.M. Qaim, A. Hermanne, M. Jahn, E. Tsyganov, N. Slavine, S. Seliounine, P.A. Antich, P.V. Kulkarni, P.E. Thorpe, R.P. Mason, F. Rösch, *Appl. Radiat. Isotopes*, 2005, **63**, 343.
- ²² L. Lattuada, A. Barge, G. Cravotto, G. B. Giovenzana, L. Tei, *Chem. Soc. Rev.*, 2011, **40**, 3019.
- ²³ C. L. Ferreira, E. Lamsa, E.; M. Woods, Y. Duan, P. Fernando, C. Bensimon, M. Kordos, K. Guenther, P. Jurek, G. E. Kiefer, *Bioconjugate Chem.*, 2010, **21**, 531.
- ²⁴ L. A. Bass, M. Wang, M. J. Welch, C. J. Anderson, *Bioconjugate Chem.*, 2000, **11**, 527.
- ²⁵ C. A. Boswell, X. Sun, W. Niu, G. R. Weisman, E. H. Wong, A. L. Rheingold, *J. Med. Chem.*, 2004, **47**, 1465.
- ²⁶ G. R. Mirick, R. T. O'Donnell, S. J. DeNardo, S. Shen, C. F. Meares, G. L. DeNardo, *Nucl. Med. Biol.*, 1999, **26**, 841.
- ²⁷ A. E. Martell, R. J. Motekaitis, E. T. Clarke, R. Delgado, Y. Sun, R. Ma, *Supramol. Chem.*, 1996, **6**, 353.
- ²⁸ G. Schwarzenbach, *Analyst*, 1955, **80**, 713.
- ²⁹ M. K. Moi, C. F. Meares, M. J. Call, W. C. Cole, S. J. DeNardo, *Anal. Biochem.*, 1985, **148**, 249.
- ³⁰ O. L. Samoiloova, V. G. Yashunskii, Patent application SU 144479, From Byul. Izobret. 1962, No. 3, 14.
- ³¹ L. H. Hall, J. J. Spijkerman, J. L. Lambert, *J. Am. Chem. Soc.*, 1968, **90**(8), 2044.
- ³² G. Anderegg, P. Nageli, F. Muller, G. Schwarzenbach, *Helv. Chim. Acta*, 1959, **42**, 827.
- ³³ E. Haber, B. A. Khaw, US. Pat. Appl. US 1980-141053, 1980, Massachusetts General Hospital, USA.
- ³⁴ H. Stetter, W. Frank, *Angew. Chem., Int. Ed. Engl.*, 1976, 686.
- ³⁵ J. F. Desreux, *Inorg. Chem.*, 1980, **19**, 1319.
- ³⁶ G. J. Stasiuk, N. J. Long, *Chem. Commun.*, 2013, **49**, 1732.
- ³⁷ R. D. Hancock, M. P. Ngwenya, *J. Chem. Soc., Dalton Trans.*, 1987, 2911.
- ³⁸ B. M. Zeglis, J. L. Houghton, M. J. Evans, N. Viola-Villegas, J. S. Lewis, *Inorg. Chem.*, 2014, **53**(4), 1880.
- ³⁹ T. J. Wadas, E. H. Wong, G. R. Weisman, C. J. Anderson, *Chem. Rev.* 2010, **110**(5), 2858.
- ⁴⁰ Z. Cai, C. J. Anderson, J. Label, *Compd. Radiopharm.*, 2014, **57**, 224.
- ⁴¹ X. Sun, M. Wuest, Z. Dovacs, A. D. Sherry, R. Motekaitis, Z. Wany, A. E. Martell, M. J. Welch, C. J. J. Anderson, *Biol. Chem.*, 2003, **8**, 217.
- ⁴² R. Shannon, *Acta Crystallogr., Sect. A: Cryst. Phys., Diffr., Theor. Gen. Crystallogr.*, 1976, **32**, 751.
- ⁴³ C.F. Baes Jr, R.E. Mesmer, *The Hydrolysis of Cations*, 1976, Wiley, New York.

- ⁴⁴ A. E. Martell, R. M. Smith, *Critical Stability Constants, Vol. 3: Other Organic Ligands*, Plenum Press, New York, 1977.
- ⁴⁵ M. D. Bartholoma, A. S. Louie, J. F. Vallian, J. Zubieta, *J. Chem. Rev.*, 2010, **110**, 2903.
- ⁴⁶ G. E. Jackson, M. J. Byrne, *J. Nucl. Med.*, 1996, **37**, 379.
- ⁴⁷ J. F. Morfin, E. Tóth, *Inorg. Chem.*, 2011, 10371.
- ⁴⁸ D. Wild, J. B. Bomanji, P. Benkert, H. Maecke, P. J. Ell, J.-C. Reubi, M. E. Caplin, *J. Nucl. Med.*, 2013, **54**, 364.
- ⁴⁹ J. Schuhmacher, H. Zhang, J. Doll, H.R. Maecke, R. Matys, H. Hauser, M. Henze, U. Haberkorn, M. Eisenhut, *J. Nucl. Med.*, 2005, **46**, 691.
- ⁵⁰ M. Fani, M.-L. Tamma, G. P. Nicolas, E. Lasri, C. Medina, I. Raynal, M. Port, W. A. Weber, H. R. Maecke, *Mol. Pharmaceutics*, 2012, **9**, 1136.
- ⁵¹ S. Froidevaux, M. Calame-Christe, J. Schuhmacher, H. Tanner, R. Saffrich, M. Henze, A.N. Eberl, *J. Nucl. Med.*, 2004, **45**, 116.
- ⁵² S. R. Banerjee, M. G. Pomper, *Appl. Radiat. Isotopes*, 2013, **76**, 2.
- ⁵³ Y. Sun, C. J. Anderson, T. S. Pajean, D. E. Reichert, R. D. Hancock, R. J. Motekaitis, A. E. Martell, M. J. Welch, *J. Med. Chem.*, 1996, **39**, 458.
- ⁵⁴ I. Velikyan, H. Maecke, B. Langstrom, *Bioconjugate Chem.*, 2008, **19**, 569.
- ⁵⁵ J. Simecek, J. Notni, T. G. Kapp, H. Kessler, H.-J. Wester, *Mol. Pharmaceutics*, 2014, **11**(5), 1687.
- ⁵⁶ E. Boros, C.L. Ferreira, J. F. Cawthray, E. W. Price, B.O. Patrick, D. W. Wester, M. J. Adam, C. Orvig, *J. Am. Chem. Soc.*, 2010, **132**(44), 15726.
- ⁵⁷ C. F. Ramogida, C. L. Ferreira, J. F. Cawthray, C. Orvig, M. J. Adam, *Nucl. Med. Biol.* 2014, **41**(7), 632.
- ⁵⁸ J. Holub, M. Meckel, V. Kubicek, F. Rosch, P. Hermann, *Contrast media & molecular imaging*, 2014.
- ⁵⁹ M. F. Ferreira, G. Pereira, J. P. Andre, M. I. M. Prata, P. M. T. Ferreira, J. A. Martins, C. F. G. C. Geraldies, *Dalton Trans.*, 2014, **43**(21), 8037.
- ⁶⁰ M. Shokeen, C. J. Anderson, *Acc. Chem. Res.*, 2009, **42**, 832.
- ⁶¹ T. A. Kaden, *Dalton Trans.*, 2006, 3617.
- ⁶² B.M. Paterson, P. S. Donnelly, *Chem. Soc. Rev.*, 2011, **40**, 3005.
- ⁶³ E. A. Ballegeer, N. J. Madrill, K. L. Berger, D. W. Agnew, E. A. McNeil, *BMC Cancer*, 2013, **13**, 218.
- ⁶⁴ B. M. Zeglis, J. S. Lewis, *Dalton Trans.*, 2011, **40**, 6168.
- ⁶⁵ B. Guérin, S. Ait-Mohand, M.-C. Tremblay, V. Dumulon-Perreault, P. Fournier, F. Bénard, *Org. Lett.*, 2010, **12**(2), 280.
- ⁶⁶ T. M. Jones-Wilson, K. A. Deal, C. J. Anderson, D. W. McCarthy, Z. Kovacs, R. J. Motekaitis, A. D. Sherry, A. E. Martell, M. J. Welch, *Nucl. Med. Biol.*, 1998, **25**, 523.
- ⁶⁷ A. J. Chang, R. Sohn, Z. H. Lu, J. M. Arbeit, S. E. Lapi, *PLoS One*, 2013, **8**, e58949.
- ⁶⁸ J. D. Silversides, R. Smith, S. J. Archibald, *Dalton Trans.*, 2011, **40**, 6289.
- ⁶⁹ J. D. Silversides, C. C. Allan, S. J. Archibald, *Dalton Trans.*, 2007, 971.
- ⁷⁰ E. H. Wong, G. R. Weisman, D. C. Hill, D. P. Reed, M. E. Rogers, J. P. Condon, M. A. Fagan, J. C. Calabrese, K. C. Lam, I. A. Guzei, A. L. Rheingold, *J. Am. Chem. Soc.*, 2000, **122**, 10561.
- ⁷¹ J. Kotek, P. Lubal, P. Hermann, I. Cisarova, I. Lukes, T. Godula, *Chem. Eur. J.*, 2003, **9**, 233.
- ⁷² R. Ferdani, D. J. Stigers, A. L. Fiamengo, L. H. Wei, B. T. Y. Li, J. A. Golen, A. L. Rheingold, G. R. Weisman, E. H. Wong, C. J. Anderson, *Dalton Trans.*, 2012, **41**, 1938.
- ⁷³ C. A. Boswell, C. A. S. Regino, K. E. Baidoo, K. J. Wong, D. E. Milenic, J. A. Kelley, C. C. Lai, M. W. Brechbiel, *Bioorg. Med. Chem.*, 2009, **17**(2), 548.
- ⁷⁴ A. M. Sargeson, *Coord. Chem. Rev.*, 1996, **151**, 89.
- ⁷⁵ N. Di Bartolo, A. M. Sargeson, S. V. Smith, *Org. Biomol. Chem.*, 2006, **4**, 3350.
- ⁷⁶ H. C. Cai, Z. B. Li, C. W. Huang, R. Park, A. H. Shahinian, P. S. Conti, *Nucl. Med. Biol.*, 2010, **37**, 57.
- ⁷⁷ M. S. Cooper, M. T. Ma, K. Sunassee, K. P. Shaw, J. D. Williams, R. L. Paul, P. S. Donnelly, P. J. Blower, *Bioconjugate Chem.*, 2012, **23**, 1029.
- ⁷⁸ E. Mume, A. Asad, N. M. Di Bartolo, L. Kong, C. Smith, A. M. Sargeson, R. Price, S. V. Smith, *Dalton Trans.*, 2013, **42**(40), 14402.
- ⁷⁹ E. Boros, E. Rybak-Akimova, J. P. Holland, T. Rietz, N. Rotile, F. Blasi, H. Day, R. Latifi, P. Caravan, *Mol. Pharmaceutics*, 2014, **11**(2), 617.
- ⁸⁰ C. Esteves, P. Lamosa, R. Delgado, J. Costa, P. Desogere, Y. Rousselin, C. Goze, F. Denat, *Inorg. Chem.*, 2013, **52**, 5138.
- ⁸¹ S. Abada, A. Lecointre, M. Elhabiri, L. J. Charbonnière, *Dalton Trans.*, 2010, **39**, 9055.
- ⁸² S. Abada, A. Lecointre, I. Déchamps-Olivier, C. Platas-Iglesias, C. Christine, M. Elhabiri, L. Charbonnière, *Radiochim. Acta*, 2011, **99**, 663.
- ⁸³ C. Christine, M. Koubemba, S. Shakir, S. Clavier, L. Ehret-Sabatier, F. Saupé, G. Orend, L. J. Charbonnière, *Org. Biomol. Chem.*, 2012, **10**, 9183.
- ⁸⁴ E. Boros, J. F. Cawthray, C. L. Ferreira, B. O. Patrick, M. J. Adam, C. Orvig, *Inorg. Chem.*, 2012, 6279.
- ⁸⁵ L. M. P. Lima, D. Esteban-Gómez, R. Delgado, C. Platas-Iglesias, R. Tripier, *Inorg. Chem.*, 2012, **51**, 6916.
- ⁸⁶ M. Roger, L. M. P. Lima, M.; Frindel, C. Platas-Iglesias, J.-F. Gestin, R. Delgado, V. Patinec, R. Tripier, *Inorg. Chem.*, 2013, **52**, 5246.
- ⁸⁷ M. Frindel, N. Camus, A. Rauscher, M. Bourgeois, C. Alliot, L. Barré, J.-F. Gestin, R. Tripier, A. Faivre-Chauvet, *Nucl. Med. Biol.*, 2014, **41**, e49.
- ⁸⁸ S. Juran, M. Wather, H. Stephan, R. Bergmann, J. Steinbach, W. Kraus, F. Emmerling, P. Comba, *Bioconjugate Chem.*, **2009**, **20**, 347.
- ⁸⁹ P. Comba, M. Kubeil, J. Pietzsch, H. Rudolf, H. Stephan, K. Zarschler, *Inorg. Chem.*, 2014, **53**(13), 6698.
- ⁹⁰ P. Comba, S. Hunoldt, M. Morgen, J. Pietzsch, H. Stephan, H. Wadepohl, *Inorg. Chem.*, 2013, **52**(14), 8131.

- ⁹¹ T. Legdali, A. Roux, A. M. Nonat, C. Platas-Iglesias, L. J. Charbonnière, *J. Org. Chem.*, 2012, **77**, 11167.
- ⁹² A. Singhal, L. M Tóth, J. S. Lin, K. Affholter, *J. Am. Chem. Soc.*, 1996, **118**(46), 11529.
- ⁹³ A. I. Pozhidaev, M. A. Porai-Koshits, T. N. Polynova, *Zh. Strukt. Khim.*, 1974, **15**(4), 644.
- ⁹⁴ R. L. Davidovich, V. B. Logvinova, L. V. Teplukhina, *Koord. Khim.*, 1992, **18**(6), 580.
- ⁹⁵ D. Parker, K. Pulukkody, F. C. Smith, A. Batsanov, J. A. K. Howard, *J. Chem. Soc., Dalton Trans.*, 1994, **5**, 689.
- ⁹⁶ A. E. Martell, R. M. Smith, Critical Stability Constants, Plenum Press, New York, 1982.
- ⁹⁷ A. E. Martell, R. M. Smith, Critical Stability Constants, Vol. 1: Amino Acids. Plenum Press, New York, 1974.
- ⁹⁸ E. Bottari, G. Anderegg, *Helv. Chim. Acta.*, 1967, **50**(8), 2349.
- ⁹⁹ L. R. Perk, G. W. M. Visser, M. J. W. D. Vosjan, M. Stigter-van Walsum, B. M. Tjink, C. R. Leemans, G. A. M. S. van Dongen, *J. Nucl. Med.*, 2005, **46**, 1898.
- ¹⁰⁰ L. R. Perk, O. J. Visser, M. Stigter-van Walsum, M. J. W. D. Vosjan, G. W. M. Visser, J. M. Zijlstra, P. C. Huijgens, G. A. M. S. van Dongen, *Eur. J. Nucl. Med. Mol. Imaging*, 2006, **33**, 1337.
- ¹⁰¹ P. K. E. Börjesson, Y. M. S. Jauw, R. Boellaard, R. de Bree, E. F. I. Comans, J. C. Roos, J. A. Castelijns, M. J. W. D. Vosjan, J. A. Kummer, C. R. Leemans, A. A. Lammertsma, G. A. M. S. van Dongen, *Clin. Cancer Res.*, 2006, **12**, 2133.
- ¹⁰² M. A. Deri, B. M. Zeglis, L. C. Francesconi, J. S. Lewis, *Nucl. Med. Biol.*, 2013, **40**, 3.
- ¹⁰³ D. J. Vugts, G. W. M. Visser, G. A. M. S. van Dongen, *Curr. Top. Med. Chem.*, 2013, **13**, 446.
- ¹⁰⁴ C. M. van Rij, R. M. Sharkey, D. M. Goldenberg, C. Frielink, J. D. M. Molkenboer, G. M. Franssen, W. M. van weerden, W. J. G. Oyen, O. C. Boermann, *J. Nucl. Med.*, 2011, **52**(10), 1601.
- ¹⁰⁵ L. Rice, C. A. Roney, P. Daumar and J. S. Lewis, *Seminars in Nuclear Medicine*, 2011, **41**, 265.
- ¹⁰⁶ E. C. F. Dijkers, J. G. W. Kosterink, A. P. Rademaker, L. R. Perk, G. A. M. S. van Dongen, J. Bart, J. R. de Jong, E. G. E. de Vries, M. N. Lub-de Hooge, *J. Nucl. Med.*, 2009, **50**(6), 974.
- ¹⁰⁷ D. A. Heuveling, A. van Schie, D. J. Vugts, N. H. Hendrikse, M. Yaqub, O. S. Hoekstra, K. H. Karagozoglou, C. R. Leemans, G. A. M. S. van Dongen, R. de Bree, *J. Nucl. Med.*, 2013, **54**, 585.
- ¹⁰⁸ J. P. Holland, V. Divilov, N. H. Bander, P. M. Smith-Jones, S. M. Larson, J. S. Lewis, *J. Nucl. Med.*, 2010, **51**, 1293.
- ¹⁰⁹ T. K. Nayak, K. Garmestani, D. E. Milenic, M. W. Brechbiel, *J. Nucl. Med.*, 2012, **53**, 113.
- ¹¹⁰ F. Guérard, Y.-S. Lee, R. Tripier, L. P. Szajek, J. R. Deschamps, M. W. Brechbiel, *Chem. Commun.*, 2013, **49**, 1002.
- ¹¹¹ J. P. Holland, N. Vasdev, *Dalton Trans.*, 2014, **43**, 9872.
- ¹¹² E. W. Price, B.M. Zeglis, J. S. Lewis, M. J. Adam, C. Orvig, *Dalton Trans.*, 2014, **43**(1), 119.
- ¹¹³ M. A. Deri, S. Ponnala, B. M. Zeglis, G. Pohl, J. J. Dannenberg, J. S. Lewis, L. C. Francesconi, *J. Med. Chem.*, 2014, **57**, 4849.
- ¹¹⁴ M. T. Ma, L. K. Meszaros, B. M. Paterson, D. J. Berry, M. S. Cooper, Y. Ma, R. C. Hider, P. J. Blower, *Dalton Trans.*, 2015, Advance Article, DOI: 10.1039/C4DT02978J.
- ¹¹⁵ V. Kubicek, J. Havlickova, J. Kotek, G. Tircso, P. Hermann, E. Tóth, I. Lukes, *Inorg. Chem.*, 2010, **49**, 10960.
- ¹¹⁶ C. F. Ramogida, C. Orvig, *Chem. Commun.*, 2013, **49**, 4720.
- ¹¹⁷ J. P. Andre, H. R. Maecke, M. Zehnder, L. Macko, K. G. Akyel, *Chem. Commun.*, 1998, 1301.
- ¹¹⁸ P. J. Riss, C. Kroll, V. Nagel, F. Roesch, *Bioorg. Med. Chem. Lett.*, 2008, **18**, 5364.
- ¹¹⁹ K. P. Eisenwiener, P. Powell, H. R. Maecke, *Bioorg. Med. Chem. Lett.*, 2000, **10**, 2133.
- ¹²⁰ G. Ruser, W. Ritter, H. R. Maecke, *Bioconjugate Chem.*, 1990, **1**, 345.
- ¹²¹ E. A. Lewis, R. W. Boyle, S. J. Archibald, *Chem. Commun.*, 2004, 2212.
- ¹²² N. Camus, Z. Halime, N. Le Bris, H. Bernard, C. Platas-Iglesias, R. Tripier, *J. Org. Chem.*, 2014, **79**(5), 1885.
- ¹²³ "Luminescent lanthanide complexes as labels", « Encyclopedia of Metalloproteins », L. J. Charbonnière, A. Nonat, Ed. Springer, 2013, Robert H. Kretsinger, Vladimir N. Uversky, Eugene A. Permyakov
- ¹²⁴ B. P. Burke, G. S. Clemente, S. J. Archibald, *J. Label. Compd. Radiopharm.*, 2014, **57**(4), 239.
- ¹²⁵ R. Bergmann, A. Ruffani, B. Graham, L. Spiccia, J. Steinbach, J. Pietzsch, H. Stephan, *Eur. J. Med. Chem.*, 2013, **70**, 434.
- ¹²⁶ E. Mume, A. Asad, N. M. Di Bartolo, L. K. Kong, C. Smith, A. M. Sargeson, R. Price, S. V. Smith, *Dalton Trans.*, 2013, **42**(40), 14402.
- ¹²⁷ P. J. Riss, C. Kroll, V. Nagel, F. Rösch, *Bioorg. Med. Chem. Lett.*, 2008, **18**(20), 5364.
- ¹²⁸ V. Duheron, M. Moreau, B. Collin, B., W. Sali, C. Bernhard, C. Goze, T. Gautier, J.-P. P. de Barros, V. Deckert, F. Brunotte, L. Lagrost, F. Denat, *ACS Chem. Biol.*, 2014, **9**(3), 656.
- ¹²⁹ M. R. Lewis, J. Y. Kao, A. L. J. Anderson, J. E. Shively, A. Raubitschek, *Bioconjugate Chem.*, 2001, **12**(2), 320.
- ¹³⁰ I. Verel, G. W. M. Visser, R. Boellaard, M. Stigter-van Walsum, G. B. Snow, G. A. M. S. van Dongen, *J. Nucl. Med.*, 2003, **44**(8), 1271.
- ¹³¹ C. Wängler, R. Schirmacher, P. Bartenstein, B. Wängler, *Curr. Med. Chem.*, 2010, **17**, 1092.
- ¹³² Z. Miao, G. Ren, H. G. Liu, L. Jiang, Z. Cheng, *Bioconjugate Chem.*, 2010, **21**(5), 947.
- ¹³³ James C Knight, Bart Cornelissen, *Am. J. Nucl. Med. Mol. Imaging*, 2014, **4**(2), 96.
- ¹³⁴ C. Wängler, R. Schirmacher, P. Bartenstein, B. Wängler, *Curr. Med. Chem.*, 2010, **17**(11), 1092.

- ¹³⁵ K. Chen, X. Wang, W. Y. Lin, C. K. F. Shen, L. P. Yap, L. D. Hughes, P. S. Conti, *ACS Med. Chem. Lett.*, 2012, **3**, 1019.
- ¹³⁶ P. V. Chang, J. A. Prescher, E. M. Sletten, J. M. Baskin, I. A. Miller, N. J. Agard, A. Lo, C. R. Bertozzi, *Proc. Natl. Acad. Sci. USA*, 2010, **107**, 1821.
- ¹³⁷ S. B. Gopal, *Basics of PET Imaging: Physics, Chemistry, and Regulations*, 2010, March 10, Springer Science & Business Media.
- ¹³⁸ M. Conti, *Physica Medica*, 2009, **25**, 1
- ¹³⁹ D. R. Schaart, S. Seifert, R. Vinke, H. T. van Dam, P. Dendooven, H. Löhner, F. J. Beekman, *Phys. Med. Biol.*, 2010, **55**, N179.
- ¹⁴⁰ S. Gundacker, A. Knapitsch, E. Auffray, P. Jarron, T. Meyer, P. Lecoq, *NIM A*, 2014, **737**, 92.
- ¹⁴¹ T. Yamaya, N. Hagiwara, T. Obi, M. Yamaguchi, K. Kita, N. Ohyama, K. Kitamura, T. Hasegawa, H. Haneishi, H. Murayama, *IEEE Trans. Nucl. Sci.*, 2003, **50**, 1404.
- ¹⁴² W. W. Moses, S. E. Derenzo, *IEEE Trans. Nucl. Sci.*, 1994, **41**, 1441.
- ¹⁴³ Y. Shao, R. W. Silverman, R. Farrell, L. Cirignano, R. Grazioso, K. S. Shah, G. Visser, M. Clajus, T. O. Tümer, S. R. Cherry, *IEEE Trans. Nucl. Sci.*, 2000, **47**, 1051.
- ¹⁴⁴ Y. Shao, K. Meadors, R. W. Silverman, R. Farrell, L. Cirignano, R. Grazioso, K. S. Shah, S. R. Cherry, *IEEE Trans. Nucl. Sci.*, 2002, **49**, 649.
- ¹⁴⁵ P. A. Dokhale, R. W. Silverman, K. S. Shah, R. Grazioso, R. Farrell, J. Glodo, M. A. McClish, G. Entine, V.-H. Tran, S. R. Cherry, *Phys. Med. Biol.*, 2004, **49**, 4293.
- ¹⁴⁶ M. M. Ter-Pogossian, N. A. Mullani, J. Hood, C. S. Higgings, M. Currie, *Radiology*, 1978, **128**, 477.
- ¹⁴⁷ K. Shimizu, T. Ohmura, M. Watanabe, H. Uchida, T. Yamashita, *IEEE Trans. Nucl. Sci.*, 1988, **35**, 17.
- ¹⁴⁸ A. Braem, M. Chamizo Llatas, E. Chesi, J. G. Correia, F. Garibaldi, C. Joram, S. Mathot, E. Nappi, M. R. da Silva, F. Schoenahl, J. Séguinot, P. Weilhammer, H. Zaidi, *Phys. Med. Biol.*, 2004, **49**, 2547.
- ¹⁴⁹ S. Jan, J. Collot, M.-L. Gallin-Martel, F. Mayet, E. Tournefier, *IEEE Trans. Nucl. Sci.*, 2005, **52**, 102.
- ¹⁵⁰ S. Salvador, D. Huss, D. Brasse, *IEEE Trans. Nucl. Sci.*, 2009, **56**, 17.
- ¹⁵¹ S. Salvador, J. Wurtz, D. Brasse, *IEEE Trans. Nucl. Sci.*, 2010, **57**, 2468.
- ¹⁵² C. Casabella, M. Heller, C. Joram, T. Schneider, *NIM A*, 2014, **736**, 161.
- ¹⁵³ H. Hacker, A. H. Soloway, *Toxicol. Appl. Pharmacol.*, 1964, **6**, 731.